Journal of Drug Delivery Science and Technology 57 (2020) 101674

Contents lists available at ScienceDirect

Journal of Drug Delivery Science and Technology

journal homepage: www.elsevier.com/locate/jddst

Development of solid lipid nanoparticle as carrier of pioglitazone for amplification of oral efficacy: Formulation design optimization, *in-vitro* characterization and *in-vivo* biological evaluation

Sharma Shaveta[a], Jyoti Singh[a], Muhammad Afzal[b], Rupinder Kaur[a], Syed Sarim Imam[c], Nabil K. Alruwaili[d], Khalid Saad Alharbi[b], Nasser Hadal Alotaibi[e], Mohammed Salem Alshammari[f], Imran Kazmi[g], Mohd Yasir[h], Amit Goyel[a], Ameeduzzafar[d,**]

[a] *Chandigarh College of Pharmacy Landran, Mohali, Punjab, India*
[b] *Department of Pharmacology, College of Pharmacy, Jouf University, Sakaka, Saudi Arabia*
[c] *Department of Pharmaceutics, College of Pharmacy, King Saud University, Riyadh, Saudi Arabia*
[d] *Department of Pharmaceutics, College of Pharmacy, Jouf University, Sakaka, Saudi Arabia*
[e] *Department of Clinical Pharmacy, College of Pharmacy, Jouf University, Sakaka, Saudi Arabia*
[f] *Department of Pharmacy Practice, Unaizah College of Pharmacy, Qassim University, Qassim, Saudi Arabia*
[g] *Department of Biochemistry, Faculty of Science, King Abdulaziz University, Jeddah, Saudi Arabia*
[h] *Department of Pharmacy, College of Health Science, Arsi University, Asella, Ethiopia*

ARTICLE INFO

Keywords:
Optimization
Pioglitazone
Anti-diabetic activity
Biochemical study
Stability study

ABSTRACT

Pioglitazone (PGL) is a hypoglycemic therapeutic agent used in the treatment of diabetes (type 2). The present research work was designed to prepare and optimize PGL loaded solid lipid nanoparticles (SLNs). The formulation was optimized using three factors lipid (Compritol® 888 ATO - A), surfactant (tween80- B) and homogenization speed (C), and their effects were evaluated on particle size (Y_1in nm) and encapsulation efficiency (Y_2in %). The optimized formulation (PGL-SLNopt) was further evaluated for physicochemical characterization, drug release, stability study, in–vivo antidiabetic and biochemical study. The optimized formulation PGL-SLNopt prepared with the composition of Compritol® 888 ATO (4.5% w/v), tween 80 (3.0% w/v) and homogenization speed (3800 rpm). The PGL-SLNopt hasshown particle size, EE, PDI, and zeta-potential 180.65 nm, 85.34%, 0.231 and −30.7 mV, respectively. The DSC and XRD spectra did not showed any peak of PGL confirm the complete entrapment of PGL in lipid due to solubilization. PGL-SLNopt exhibited significant ($P < 0.05$) prolonged release (89.56 ± 3.11% in 12 h) than pure PGL. The anti-diabetic study indicated that PGL-SLNopt showed significantly ($P < 0.05$) higher hypoglycemic activity (57.6% reduction in 12 h) as well as improved biochemical parameters. Our finding results revealed that PGL-SLNs could be a potential delivery system for the management of diabetes (type-2).

1. Introduction

Diabetes (type-2) is defined as increase the blood glucose level (> 70–110 mg/dl) which are associated with the risk of microvascular damage like nephropathy, retinopathy, and neuropathy. The occurrence of diabetes has increased radically in the last decade and is rising rapidly in undeveloped country [1,2]. About 95% of type 2 diabetes considerably associated with elderly persons, and also arises due to the genetic character, obesity, and living lifestyle [3]. There are several anti-diabetic drugs currently used for the management of diabetes (type 2), and mechanism includes, i.e., enhancing secretion of insulin, reducing insulin resistance, and preventing reabsorption of glucose from loop of Henley [4].

Pioglitazone (PGL) is an oral anti-hyperglycemic drug and chemically belong to thiozolidindione (Glitazones) category (Fig. 1). It improves the insulin resistance as well as decreases macrovascular risk in diabetic patients [5]. It significantly decreases the glycosylated hemoglobin (HbA1c), reduces fasting and postprandial blood glucose levels, as well as improves beta-cell function [6]. PGL belongs to Class II of biopharmaceutical classification system (BCS), i.e., low soluble (1.8 μg/mL), high permeable and also have short half-life (3–6 h) [7]. The low water solubility indicates the dissolution is the rate-limiting

* Corresponding author. Assistant Professor Department of pharmaceutics, College of Pharmacy Jouf University, Sakaka, Al-Jouf, Saudi Arabia.
E-mail address: zzafarpharmacian@gmail.com (Ameeduzzafar).

https://doi.org/10.1016/j.jddst.2020.101674
Received 6 January 2020; Received in revised form 6 March 2020; Accepted 14 March 2020
Available online 23 March 2020
1773-2247/

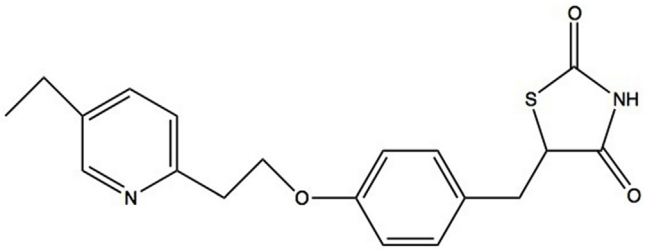

Fig. 1. Chemical structure of pioglitazone.

step that shows poor absorption and leads to reduction in pharmacological activity. Consequently, this may reflect in the increased dose and associated adverse side effects. Many drug delivery systems include nano lipid formulations [8–10], gastro retentive formulation [11], and self-emulsifying systems [12], have been reported for enhanced therapeutic efficacy of PGL.

There are various lipid based nanoformulations have been investigated by the researchers for the enhancement of solubility, dissolution and absorption profile of poorly soluble drugs [13–16]. The SLNs have nano size, unique structure properties, high drug loading and biocompatibility [17,18]. It is composed of physiological or biocompatible lipids core entrapped with lipophilic drug and surfactant at the outer shell [19]. It increases the bioavailability of lipophilic drugs as well as achieves the desired concentration at the receptor site. It has high drug loading and encapsulation capacity for both hydrophilic and lipophilic therapeutics as well as high resistance in the gastric environment due to their nano size ranges. It has the ability to transport through the lymphatic system. SLNs evade the efflux transporter protein (P-glycoprotein, P-gp) and improve the permeability of therapeutics [20]. The SLNs assist the intestinal permeability as well as absorption by avoiding the first-pass metabolism. It protects drug degradation from the acidic environment and enhances the drug absorption to the systemic circulation [21]. The number of responses like particle size, EE, release, loading efficiency significantly effects on the physicochemical properties of the SLNs [22].

There are different statistical designs (Box Behnken design, Taguchi, D-Optimal, Placket Burman, 2-level factorial) applied by many researchers reported for formulation optimization [23,24]. BBD design is a novel tool for formulation optimization because it gives lowers number of trials and less time consuming. The aim of the response surfaces methodology to understand the effects of fundamental factors on the response and to achieve appropriate formulations with target goals [25].

The objective of the present research work was to develop PGL loaded SLN (PGL-SLNs) by hot homogenization method. The prepared formulations were statistically optimized by applying three-factor and three-level BBD. Compritol® 888 ATO (A), tween 80 (B), and homogenization speed (C) used as an independent variables and their effects evaluated on dependent variables like particle size (Y_1) and EE (Y_2). The optimized formulation (PGL-SLNopt) formulation will be further assessed for solid-state characterization, drug release, in-vivo anti-diabetic and biochemical evaluation in albino Wistar rat model.

2. Materials and methods

2.1. Materials

Pioglitazone procured from Aurobindo Pharma Ltd (Hyderabad India). Precirol® ATO5 and Compritol® 888 ATO received from the Gattefosse (Mumbai, India). Glycerol monosterate (GMS), stearic acid (SA), and cetostearyl alcohol (CSA) were procured from Acros organic (New Jersey, USA). Tween 80, methanol and chloroform were procured from Mohini Organics Pvt. Ltd. (Mumbai, India). Other chemicals were used during the study were of analytical grade and Milli-Q water used throughout the study.

2.2. Method

2.2.1. Partitioning behavior

The selection of solid lipid for PGL-SLNs was done on the basis PGL solubility in the solid lipids [26]. The solubility of PGL was determined in various solid lipids, i.e., Precirol® ATO5, Compritol® 888 ATO, glycerol monosterate (GMS), stearic acid (SA), and cetostearyl alcohol (CSA). The precise quantity of PGL (15 mg) was added in a mixture of melted solid lipid (2 g m) and hot double distilled water (3 mL). The sample was mechanically shaken on a water bath shaker at 80 °C for 30 min. The mixture was centrifuged at 6000 rpm (Remi centrifuge) for 10 min and aqueous phase was separated. PGL concentration in the aqueous phase was analyzed by UV-spectrophotometer (U·V-1800, Shimadzu, Japan) after appropriate dilution in triplicate.

2.2.2. Preparation of solid lipid nanoparticles

Hot homogenization technique was employed for development of

Table 1
Formulation composition of pioglitazone solid lipid nanoparticles using Box Behnken design based independent variables and their effect on dependent variables (actual and predicted value).

Std order	Lipid (% w/v)	Surfactant (%) w/v	Homogenization speed (rpm)	Particle size (nm)		Entrapment efficiency (%EE)	
				Actual value	Predicted value	Actual value	Predicted value
1	2.00	1.00	4000	226.02	226.39	67.41	67.34
2	6.00	1.00	4000	249.54	250.07	92.32	92.36
3	2.00	4.00	4000	103.32	102.79	56.03	56.00
4	6.00	4.00	4000	213.04	212.67	75.21	75.28
5	2.00	2.50	3000	178.43	178.65	69.51	69.65
6	6.00	2.50	3000	242.34	242.40	88.86	88.89
7	2.00	2.50	5000	125.24	125.18	57.43	57.40
8	6.00	2.50	5000	195.21	194.99	82.59	82.45
9	4.00	1.00	3000	268.43	267.84	86.34	86.27
10	4.00	2.50	4000	176.09	176.40	69.11	69.01
11	4.00	1.00	5000	206.76	206.45	73.77	73.87
12	4.00	4.00	5000	136.32	136.91	62.65	62.72
13	4.00	2.50	4000	184.64	184.25	75.87	75.65
14	4.00	2.50	4000	183.65	184.25	75.34	75.65
15	4.00	2.50	4000	186.32	184.25	75.15	75.65
16	4.00	2.50	4000	183.76	184.25	76.04	75.65
17	4.00	2.50	4000	182.86	184.25	75.86	75.65

Lipid: Compritol® 888 ATO; Surfactant: tween 80.

PGL-SLNs formulations. From the preliminary study, Compritol® 888 ATO was selected as solid lipid and tween 80 as surfactant [27]. The detailed composition of prepared PGL-SLNs have been shown in Table 1. The calculated quantity of PGL (15 mg) and lipid (quantity shown in Table 1) were dissolved in the organic solvent. The organic solvent was evaporated and the drug lipid mixture was melted above (5 °C) the melting temperature of lipid. The aqueous surfactant (tween 80) solution was prepared separately, heated at same temperature of lipid phase (70 °C) and added drop-wise into lipid phase with continuous stirring. The prepared dispersion was sonicated for 5 min to get a pre-emulsion and then placed into hot high-pressure homogenization (IKA® T25 digital ULTRA-TURRAX®, Germany) at 12,000 × *g* for 20min to reduce the size. Finally, the prepared samples were cooled at room temperature and the formation of SLNs takes place. The sample stored at 4 °C for further study.

2.2.3. Optimization

The three-factor and three-level BBD was employed for the optimization of PGL-SLNs using Compritol® 888 ATO (A), tween 80 (B), and homogenization speed (C) as independent variables. The total seventeen experimental runs were obtained with different independent levels as low (−1), medium (0), and high (+1) (Table 1). The particle size (Y_1) and EE (Y_2) were selected as independent responses. All the responses of each runs were concurrently fitted to linear, 2F1, and quadratic models for determination of best fitted model. The contour and 3D-plots were created by the software and used for the evaluation independent factor over each response. The actual value of each response quantitatively compared to the predicted values obtained from software. The general polynomial equation for quadratic model was generated by the BBD to check the effect of independent variables over the response. The general polynomial equation was given bellow.

$$Y = b_0 + b_1A + b_2B + b_3C + b_{12}AB + b_{13}AC + b_{23}BC + b_{11}A^2 + b_{22}B^2 + b_{33}C^2 + \text{———————}$$

Where, Y is the response b0 was an intercept, b_1, b_2, and b_3 are linear coefficients, b_{11}, b_{22}, and b_{33} are squared coefficients and quadratic term, b_{12}, b_{13}, and b_{23} were interaction coefficients between two variables simultaneous. To assess the best fit model, predicted R^2 and adjusted R^2 values were evaluated to select the model [28,29].

2.3. Characterization

2.3.1. Particle size, PDI and zeta potential

The particle size, PDI and zeta-potential of PGL-SLNs were analyzed by zeta sizer (Malvern zeta sizer- 1000 HS, Malvern UK). PGL-SLNs were diluted in an appropriate solvent (100 fold) and observed through a laser (50 mV) light scattering at a 90° fixed angle in triplicate.

2.3.2. Encapsulation efficiency

The ultracentrifugation technique used to estimate the encapsulation efficiency of PGL-SLNs dispersion. The PGL-SLNs were filled into centrifugation tubes and centrifuged at 18,000 rpm using cooling centrifuge (Sigma 3-1 KL IVD, Germany) for 30 min. The supernatant was collected and PGL concentration was analyzed by UV spectrophotometer at 220 nm in triplicate after appropriate dilution. The % EE calculated by given equation:

$$\%\ EE = \frac{\text{Concentration of PGL in supernatant}}{\text{Initial PGL concentration}} \times 100$$

2.3.3. Drug loading

The drug load of optimized formulation (PGL-SLNopt) was determined by centrifugation method. The sample was placed in centrifugation tube and centrifuged at 18,000 rpm using cooling centrifuge (Sigma 3-1 KL IVD, Germany) for 30 min. The supernatant was collected and SLN pellet was washed with distilled water and dispersed in a methanol. Then it was sonicated using probe sonicator for 15min and the resulting sample was again centrifuged at 18,000 rpm. Finally, the supernatant was collected and PGL content was determined by UV spectrophotometer at 220 nm in triplicate. The drug loading was calculated by following formula

$$\text{Drug loading}\ (\%) = \frac{nconcetration\ of\ PGL\ in\ SLN}{total\ weight\ of\ SLN} \times 100$$

2.3.4. Transmission electron microscope

The morphological examination of PGL-SLNopt was examined by a Transmission electron microscope (TEM, H100, Hitachi, Japan). A small drop of PGL-SLNopt was taken on the carbon-coated copper grid and phosphotungstic acid (2% v/v) was added to stain the sample. The sample incubated for 10 min, and excess was removed with cotton/filter paper. The stained and dried sample positioned in the electron microscope for the analysis, the image was captured and analyzed by an electron microscope.

2.3.5. Differential scanning calorimetry

The thermal spectra of PGL, Campritol ATO888 and PGLSLNopt were taken by using a differential scanning calorimeter (Perkin-Elmer, DSC 821, Mettler Toledo, Switzerland). The samples (4 mg) were filled in an aluminium pan and evaluated under nitrogen stream by applying pressure. The scanning performed at a temperature range of 40–200 °C with 10 °C/min constant heating rate.

2.3.6. X-ray powder diffraction

The crystallinity of the PGL, Campritol ATO888 and PGL-SLNopt were evaluated by an X-ray diffractometer (XPERT-PRO, PAN analytical, Netherlands). The patterns were recorded at two theta range 0-70° (2Θ, 0.5°/min) with the tube voltage (40 Kv) and tube current (40 mA) in step mode.

2.3.7. Fourier transforms infrared spectroscopy

The FTIR spectral analysis of PGL, Campritol ATO888 and PGL-SLNopt were performed using FT-IR spectrophotometer (Perkin- Elmer, USA). The samples were evaluated in the scanning range 4000–400 cm^{-1} with 4 cm^{-1} resolution.

2.3.8. In-vitro drug release

The dialysis bag technique was used to check the release study of PGL-SLNopt and pure PGL dispersion [30]. The samples of pure PGL and PGL-SLNs dispersions (equivalent to 2.0 mg PGL) was filled into dialysis bag and sealed from both ends. It was immersed into of 0.1 *N* HCl (500 mL) as release media for 2 h then transferred to phosphate buffer saline (500 mL, pH 7.4). The media was continuously stirred at 50 rpm and temperature was set at 37 °C ± 0.5 °C throughout the study. The aliquot (5 mL) was withdrawn at specific time intervals and same volume replaced with fresh released media to maintain the concentration gradients. The concentration of PGL was determined at each time point using UV- spectrophotometer and amount of PGL released was calculated. The released data was fitted into various kinetic release model equations for the determination of best-fit release model for PGL-SLNopt.

2.4. In-vivo study

2.4.1. Animal handling

The preclinical study of PGL-SLNopt and pure PGL assessed on healthy male albino Wistar rats (150–200 g m). All animal experiments performed in conformity with National Institutes of Health guide for the care and use of laboratory animal (NIH Publications No. 8023, revised 1978). The protocol of preclinical study was evaluated and approved by the institutional animal ethics committee (IAEC), Chandigarh College of Pharmacy Landran, Mohali, Punjab, India. The rats were procured from

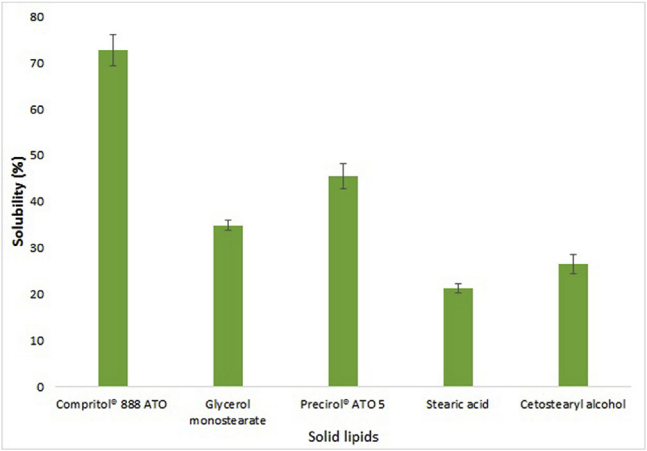

Fig. 2. Solubility study of pioglitazone in different solid lipids.

the animal house and kept under 12 h dark/light cycles at standard environmental conditions. The blood glucose levels (BGL) of each animal was measured before the study. The experimental animals fed with fat rich diet (powdered normal pellet diet, casein protein, coconut oil, vitamin, cholesterol, sodium chloride, sucrose, fructose, and DL-methionine) for 15 days before the induction of diabetic. The rats were randomly selected and divided into four groups and each group having six rats. The group-1 taken as normal control, group-2 taken as disease control, group-3 treated with PGL-SLNopt formulation, and group-4 treated with pure PGL dispersion.

2.4.2. Induction of diabetes

The diabetes in the albino rats was induced by administration of high-fat diet-and intraperitoneal administration of single low dose (35 mg/kg) streptozotocin [31]. After 72 h of streptozotocin administration, the fasting BGL was measured by a digital glucometer (Accu Check, Roche, Germany). The fasting BGL ≥220 mg/dL were considered as diabetic condition and taken for experimental study.

2.4.3. Assessment of anti-diabetic activity

The animals treated with PGL-SLNopt (group 3) and pure PGL dispersion (group 4) treated orally with PGL equivalent to 30 mg/kg body weight. At fixed time intervals (0,1, 2, 4, 8, 12 and 24 h) the BGL was measure by digital Accu-Check glucometer. A drop of blood was taken from rat tail and placed into glucometer strip. After few second the BGL displayed on screen of digital glucometer was noted down. The evaluation was continued till 24 h and the % reduction in BGL determined by the given formula:

$$\%\ \text{Reduction in BGL} = \frac{BGL_{t\to 0} - BGL_{t\to t}}{BGL_{t\to 0}} \times 100$$

2.4.4. Biochemical study

After completion of study, the blood samples were collected in eppendorf tube from retro-orbital plexus in anaesthetized condition. The light dose of diethyl ether used as anesthetic agent. The blood samples were stand for 30 min without any disturbance and centrifuged at 3000 rpm for 15 min. The clear supernatant blood serum was separated and placed into refrigerator at 2–4 °C. The liver function test (SGOT & SGPT), kidney function test (urea & uric acid) and lipid profile (total cholesterol, triglyceride, HDL), and liver were analyzed by PAP method using the standard kits [32].

2.5. Stability study

The storage stability study of PGL-SLNopt was evaluated as per ICH guidelines [33]. The PGL-SLNopt (10 mL) filled into the borosilicate glass vials and stored at 25 ± 0.5 °C/60% and 40 ± 0.5 °C/75%RH for six months in the humidifier stability chamber (Thermo Scientific, Sweden). After a definite time interval (1, 2 3 and 6 months), each sample was withdrawn and analyzed for particle size and encapsulation efficiency.

2.6. Statistical analysis

All the values were represented as the mean ± SD of three independent replicates. The Graph-pad Instat Software (San Diego, CA, USA) was applied for data analysis. One way ANOVA and Tukey-Kramer, multiple comparisons test was applied for determination of significant level. The $P < 0.05$ value considered for statistical significance.

3. Result and discussion

3.1. Partitioning behavior

The amount of PGL dissolved in the different solid lipid was calculated and data shown in Fig. 2. The distribution coefficient of PGL in each phase system was determined and found to be in the sequence of Compritol® 888 ATO (72.76 ± 3.34%) > Precirol® ATO 5 (45.45 ± 2.67) > glycerol monostearate (34.87 ± 1.12) > cetostearyl alcohol (26.46 ± 2.05) > stearic acid (21.32 ± 0.98). Based on the highest partitioning of PGL, Compritol® 888 ATO was selected as a best solid lipid for the preparation of PGL-SLNs.

3.2. Optimization

The formulation was optimized by using Box Behnken design (BBD). The independent variables were chosen on the basis of a preliminary experimental study results. The optimization results showed 103.32 nm–268.43 nm for particle size and 56.03–92.32% for EE (Table 1). It was observed that best-fitted model was quadratic for each response, i.e., particle size and %EE. The high R^2 value observed for quadratic model than the other model. The polynomial equations (quadratic) of each response generated from software given below:

Particle size (Y_1) = +184.25 + 33.39*A- 40.25*B- 25.22*C+ 21.55*A*B+1.52*A*C+ 5.48* B*C+ 1.07*A^2+ 12.66*B^2- 0.010*C^2 (equation-1).

Encapsulation efficiency (Y_2) = +75.65 + 11.07*A - 7.10*B - 4.67*C- 1.43*A*B + 1.45*A*C + 1.53*B*C - 0.64*A^2-2.27*B^2- 0.41*C^2 (equation-2). Where, A, B and C are coded values of the lipid (Compritol® 888 ATO), surfactant (tween 80) and homogenization speed. The positive sign indicates the positive to effect, whereas negative sign showed a negative effect on dependent variables or responses. The lack-of-fit for all responses were found to be not significant ($P > 0.05$) at 95% confidence level. Moreover, the remaining parameters of the quadratic model were found to be significant ($P < 0.0001$) with high F-value and high value of "Adeq Precision" (> 4). It indicates that the model was well fitted with adequate signal. The predicted and actual value of all responses of each experimental run was expressed in Table 1.

3.2.1. Effect of independent variables on particle size

The particle size of PGL-SLNs was found in the range of 103.32 nm–268.43 nm. The polynomial equation (eq-1), 3D plot and contour plot explained the effect of variable on particle size (Fig. 3A). The lipid has shown an agonistic effect on SLN size. As concentration of lipid increases from 2 to 6%, the SLNs size was increases. The increase in size takes place due to the aggregation of particles. The second-factor i.e., surfactant (tween 80) has a negative effect on the particle size, i.e., an increase in concentration from 1 to 4%, the SLNs size was decreases. The decrease in size may be due to the reduction in interfacial tension between two phases which retard the agglomeration of particles

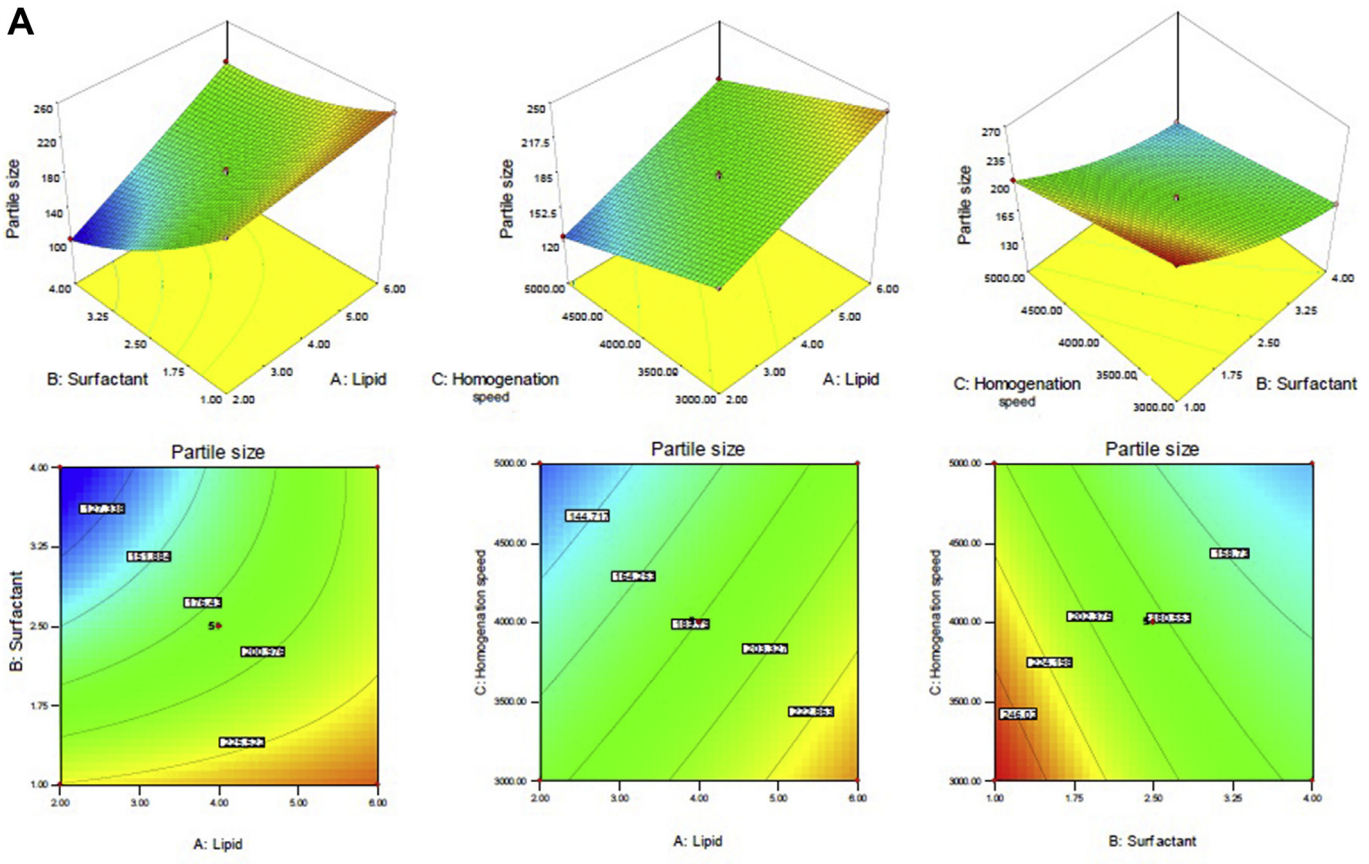

Fig. 3A. Effect of compritol® 888 ATO (A), tween 80 (B), homogenization speed (C), on particle size (Y_1).

[34,35]. The homogenization speed helps to break the particle. As the homogenization speed increases, the SLNs size decreased due to breakdown of particles into smaller size [36].

3.2.2. Effect of independent variables on EE

The EE of each experimental run of PGL-SLNs estimated by the centrifugation technique and the results depicted in Table 1. EE was found in the range of 56.03–92.32%, and the effects of variables on the EE were expressed by polynomial equation (eq-2), 3D plot and contour plot (Fig. 3B). The increase in concentration of lipid from 2% to 6% leads to an increase in EE. The increase in EE is due to the greater space available to entrap the PGL in to lipid matrix. The surfactant (Tween80) showed biphasic behavior on EE. The initial increase in concentration leads to enhancement in the EE because of higher solubility of PGL and reduction in the partition of a drug in the aqueous phase [37]. The further increase in the concentration leads to the formation of the micelle and the solubility of PGL in the water phase system was also increased, and EE decreased. The increase in the homogenization speed leads to the breakdown of particles and the leaching of the drug take place, due to which the EE (%) decreased [38,39].

3.2.3. 3D-response surface and contour plot

A total of 17 experimental runs were obtained from BBD optimization software using three factors at three levels and data were depicted in Table 1. The effects of independent variables on one response at one time expressed by 3D and contour plots which are were generated by BBD software (Fig. 3A and B). The values of various statistical parameters like Sum of squares, Degrees of freedom (df), Mean squares, F-value, P-value, R^2, coefficient of variances (CV), standard deviation (SD) for regression, lack of fit and residual of the best fitted quadratic model given in Table 2. The statistical summary (R^2, Adjusted R^2, and Predicted R^2) of each model, i.e., Linear, 2FI and Quadratic model of both responses given in Table 3. A significant variation in R^2, Adjusted R^2, and Predicted R^2 value was obtained for all models of each response and $R^2$was found to be maximum for the quadratic model. So that quadratic model was considered as the best fit model for each response. The results of response-fitting designate the optimized PGL-SLNs with high % EE, optimum average particle size. The optimized formula of SLNs obtained from point prediction of BBD software having the composition of lipid concentration (Compritol® 888 ATO - 4.5% w/v), surfactant (tween 80–3.0% w/v) and homogenization speed (3800 rpm). The actual and predicted value of particle size and EE of PGL-SLNopt was found to be 180.65 nm (Fig. 4A), and 184.25 nm, 85.34% and 82.65%, respectively. The closeness of predicted and actual value of these results showed the robustness of the optimization method used for preparation the PGL-SLNs. The PDI, zeta-potential and drug load of PGL-SLNopt formulation was found to be 0.231, −30.7 mV (Fig. 4B), and 12.5 ± 0.98% respectively.

3.3. Transmission electron microscope

The shape and surface morphology of PGL-SLNopt was done through TEM and the image exhibited spherical shape with smooth surfaces without any aggregation (Fig. 5).

3.4. Differential scanning calorimetry

Thermal behavior study of PGL, lipid and PGL-SLNopt performed throughDSC and thermogram was shown in Fig. 6. The thermal spectra of PGLand lipidexhibited a sharp endothermic peak at 185 °C and 75.5 °C, respectively, which is corresponding to its melting point. The thermal spectra of PGL-SLNopt did not exhibit an endothermic melting peak of PGL and showed a melting peak of Compritol® 888 ATO at 65.3 °C. The endothermic peak of Compritol® 888 ATO in PGL-SLNopt

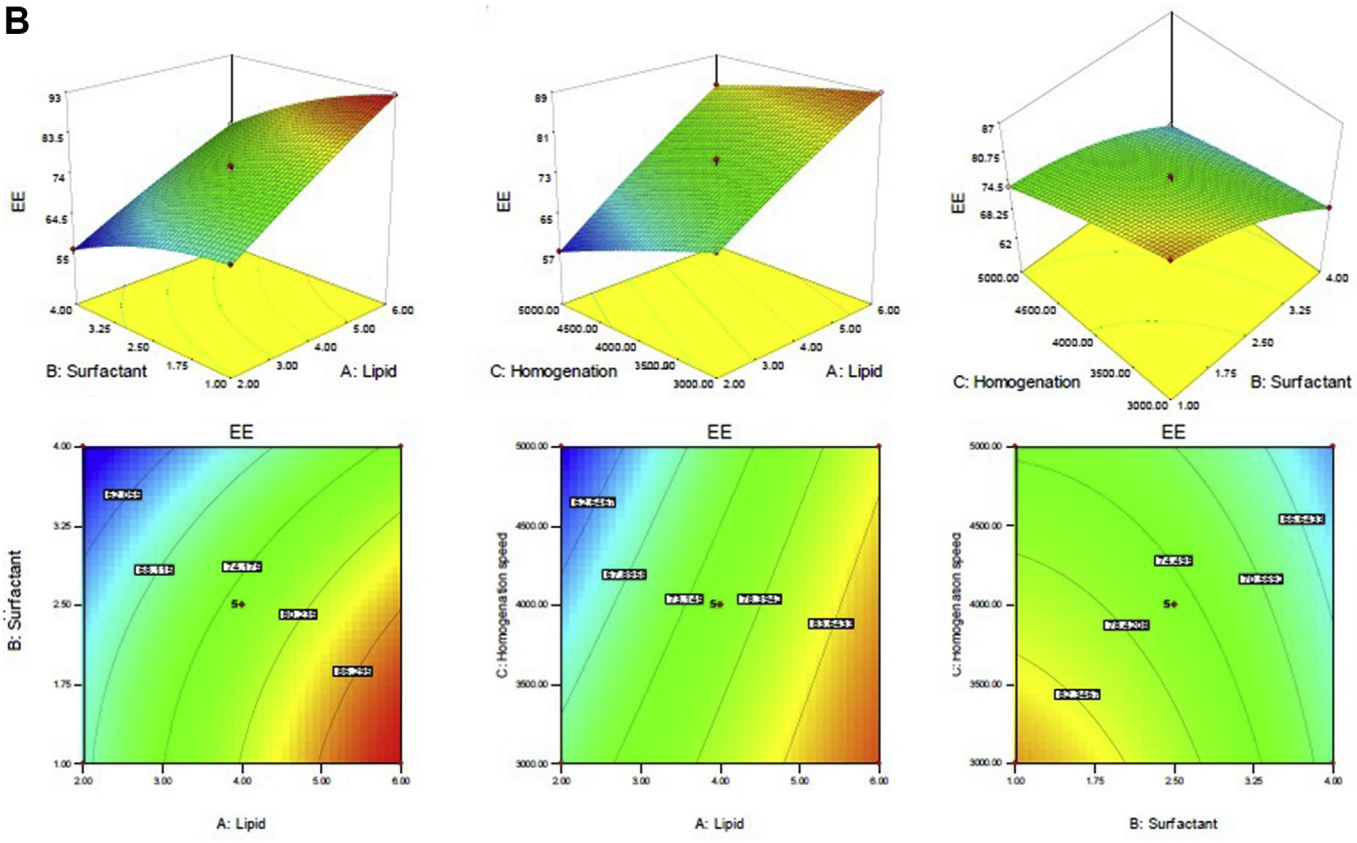

Fig. 3B. Effect of Compritol® 888 ATO, (A) tween 80, (B) and homogenization speed, (C) on encapsulation efficiency (Y_2).

Table 2
ANOVA value of dependent variables of pioglitazone solid lipid nanoparticles.

Result (ANOVA)	Particle size	Entrapment efficiency
Regression		
Sum of squares	29643.56	1611.26
Degrees of freedom (df)	9	9
Mean squares	3293.73	179.03
F-value	2626.23	1862.17
P	< 0.0001	0.0001
Lack of fit tests		
Sum of squares	1.81	0.082
Degrees of freedom (df)	3	3
Mean squares	0.60	0.027
F-value	0.35	0.19
P	0.7949	0.9009
R^2	0.9997	0.9996
Correlation of variation (% CV)	0.59	0.42
Residual		
Sum of squares	8.78	0.67
Degrees of freedom (df)	7	7
Mean squares	1.25	0.096

Table 3
Statistics model summary of responses of pioglitazone solid lipid nanoparticles.

Model	R^2	Adjusted R^2	Predicted R^2	SD	% CV	Remark
Response (Y_1)						
Linear	0.9094	0.8885	0.8174	14.37	–	–
2FI	0.9764	0.9623	0.9080	8.36	–	–
Quadratic	0.9997	0.9993	0.9987	1.12	0.59	Suggested
Response (Y2)						
Linear	0.9676	0.9602	0.9399	2.00	–	–
2FI	0.9837	0.9740	0.9484	1.62	–	–
Quadratic	0.9996	0.9990	0.9986	0.31	0.42	Suggested

slightly shifted towards the lower melting temperature. The shifting to the lower melting temperature of Compritol® 888 ATO is due to a nanosize particle range. It increases the surface area leading to decrease in the melting point as compared to Compritol® 888 ATO. Because the large crystal required more energy and takes a long time for melting. This is also due to the presence of a surfactant (tween 80) and dispersed state of Compritol® 888 ATO. The absence of drug peaks in SLNs spectra indicatesthe complete drug entrapment in the lipid matrix due to amorphization. The result agreed to previously published results [6,20,39].

3.5. *X-ray powder diffraction*

XRD spectra of pure PGL, Compritol® 888 ATO and PGL-SLNopt were studied and shown in Fig. 7. The pure PGL spectra showed intense characteristics peak at 2 theta diffraction angles, i.e., 10.1, 16.2, 19.5 and 23.7, confirmed crystalline nature of PGL. The Compritol® 888 ATO exhibited characteristic lattice at 2° theta diffraction angles of 20.6 and 24.8. The XRD spectra of PGL-SLNopt did not showed any characteristic peak of PGL, only the peaks of Compritol® 888 ATO was found at 2° theta diffraction angles, i.e., 20.9 and 24.9. This finding can be observed due to the nanosize range of SLNs, encapsulation and solubilization of PGL in the lipid matrix as well as amorphization of the PGL in lipid matrix [40].

3.6. *Fourier-transform infrared spectroscopy study*

The FT-IR spectral analysis of PGL, Compritol ATO888, and PGLSLNopt, were measured to evaluate the compatibility. The FTIR spectra of PGL exhibited characteristic N–H stretching peak at 3079 cm^{-1}, C–H stretching peak at 2989 cm^{-1}, C= O stretching peak at 1738 cm^{-1}, C=C (aromatic) stretching at 1603 cm^{-1} and C–S peak at 1223 cm^{-1}. The FTIR spectra of PGL-SLNopt showed the

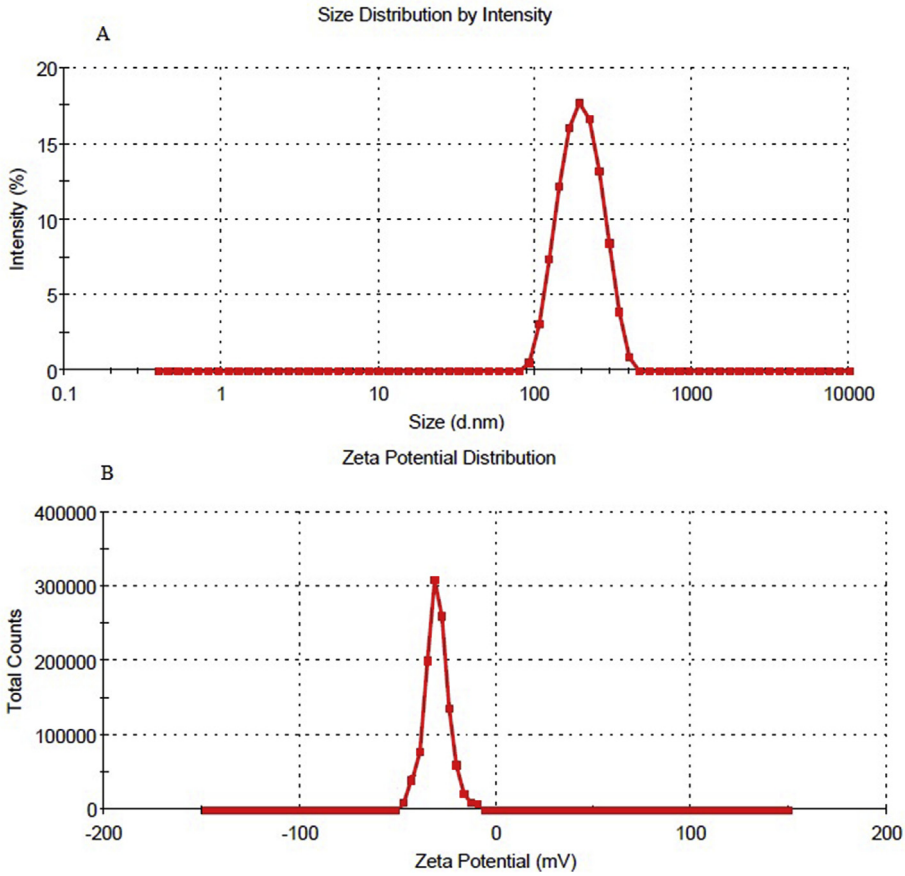

Fig. 4. Optimized pioglitazone solid lipid nanoparticles (A) Particle size, (B) Zeta potential.

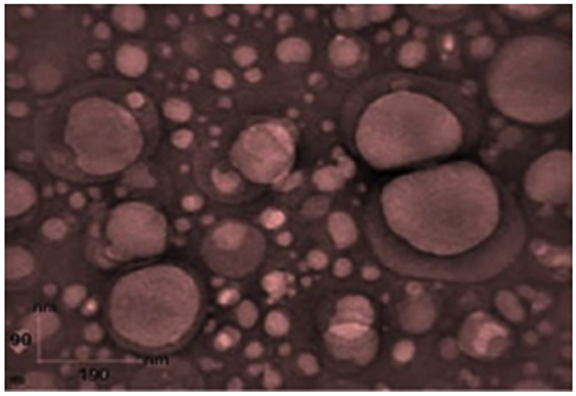

Fig. 5. Transmission electron microscopy image of optimized pioglitazone solid lipid nanoparticles (PGL-SLNopt).

characteristic N–H stretching peak at 3079 cm^{-1}, C–H stretching peak at 2989 cm^{-1}, C= O stretching peak at 1738 cm^{-1}, aromatic C=C stretching at 1600 cm^{-1} and C–S peak at 1223 cm^{-1}. The intact peak of Campritol ATO888 and PGL was also present in the PGL-SLNopt spectra. This finding concluded that PGL was compatible to SLNs components (no interaction).

3.7. In-vitro drug release

The release of PGL from PGL-SLNopt was analyzed and compared with the release pattern of pure PGL in the same condition. PGLSLNopt displayed higher and prolonged-release, i.e., 89.56 ± 3.11% in 12 h of study whereas, pure PGL showed the poor release pattern, i.e., 43.12 ± 2.11% (Fig. 8). The release of PGL from PGLSLNopt exhibited a dual release profile, initial burst release within 2 h, followed by a sustained release pattern [41]. This type of release behavior achieved due to quick release of PGL adsorbed on the SLNs surface. In later stage the prolonged drug release achieved due to solubilized or dispersed PGL releases slowly from the inside of lipid core matrix by diffusion mechanisms. The SLN showed significantly higher drug release due to the presence of Compritol® 888 ATO as solid lipid and tween 80 as a surfactant which helps to improve the release of the weakly soluble therapeutics. The release data was fitted into different release kinetic model. The korsmeyer-Peppas model was found as the best fit release model because it has shown maximum R^2. It indicates release mechanism followed controlled through diffusion followed by erosion of lipid matrix.

3.8. In-vivo study

3.8.1. Anti-diabetic assessment

The comparative anti-diabetic effect of pure PGL and PGL-SLNopt was evaluated into STZ (low dose) induced diabetes Wistar albino rats and the results depicted in Fig. 9. The baseline of BGL in normal control (Group 1) was 111.56 ± 4.23 mg/dL whereas diabetic control group showed 220.38 ± 6.11 mg/dL, respectively. PGL-SLNopt (group 3) treated rats showed a significant reduction in BGL up to 12 h. The highest reduction in BGL observed in PGL-SLNopt treated group i.e., 51.2% (122 ± 6 mg/dL) at 12 h, whereas the pure PGL dispersion treated group animal showed a maximum reduction in BGL 44.4% (139 ± 7 mg/dL) at 4 h. It indicates that PGL-SLNopt showed significantly ($P < 0.001$) superior hypoglycemic activity than pure PGL dispersion. It confirms that PGL has higher therapeutic effectiveness after encapsulating it into SLN formulation. The enhancement of absorption of PGL in SLN formulation could be due to the amplification of

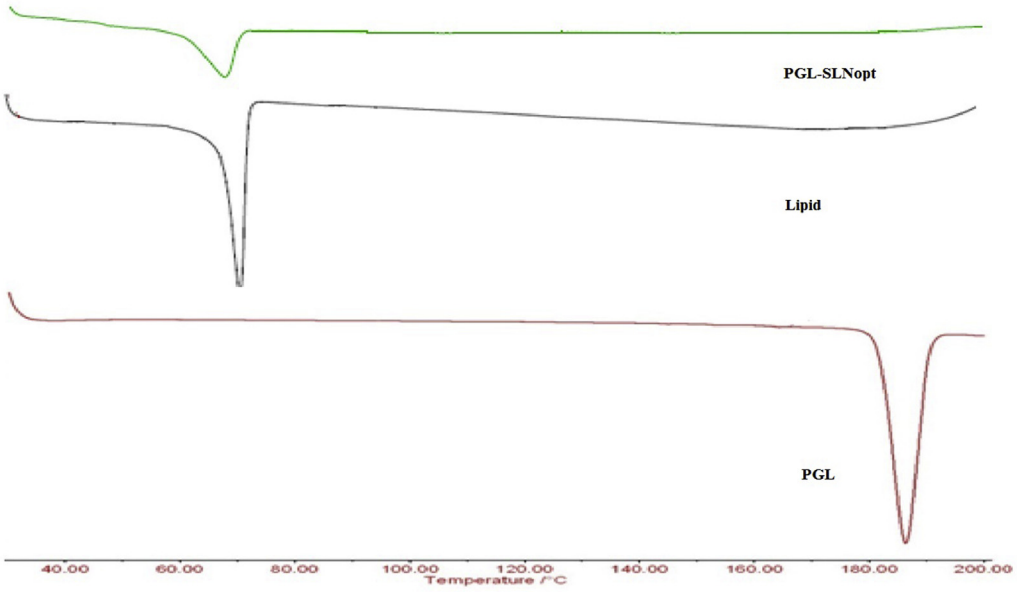

Fig. 6. Differential scanning calorimetry image of PGL, Campritol ATO888 and optimized pioglitazone solid lipid nanoparticles (PGL-SLNopt).

lymphatic transport of drug. The external lipid base formulation increases lymphatic transport by the formation of lipoprotein and intestinal lymphatic lipid flux [42,43].

3.8.2. Biochemical study

The serum biochemical parameters estimated using standard kits. The levels of total cholesterol (TC) and triglyceride (TG) significantly reduced ($P < 0.001$) whereas H-DLC levels significantly ($P < 0.001$) increased after the treatment with pure PGL and PGL-SLNopt than diabetic control rats (Table 4). The SGOT and SGPT levels reduced significantly ($P < 0.001$) after treatment with, PGL and PGL-SLNopt as compared to diabetic controls. In addition, PGL-SLNopt significantly ($P < 0.01$) reduced serum SGOT levels as compared to pure PGL treated group. The serum uric acid levels did not change significantly ($P > 0.05$, #ns) in pure PGL treated rats. PGL-SLNopt treated rats showed a significant reduction ($p < 0.01$) in comparison to the diabetic control group. The study indicates that pure PGL and PGL-SLNopt significantly improved biochemical alteration. The insulin derangements are mainly responsible for variation in the lipid profile, which contributes to cardiovascular complications associated with diabetes [44]. Due to liver toxicity of STZ in rats, the enormous secretion of liver enzymes takes place, which restored towards normal value with PGL-SLNopt treatments [45]. These result agreed to previously published results [40,42,43].

3.9. Stability study

The stability result of PGL-SLNopt at room and accelerated condition as per ICH guidelines was depicted in Fig. 10A and B. After storage for six months, the sample analyzed at different time intervals and found an increase in particle size and decrease in EE on storage at room and accelerated condition. The initial particle size and EE noted as 183.65 ± 3.43 nm and 85.34 ± 4.11%, and after 180 days at 25 °C/60%RH, the size and encapsulation efficiency were reached to 210.65 ± 4.43 nm and 78.42 ± 3.98%, respectively. The result of particle size and EE of PGL-SLNopt dispersion stored at 40 °C found significantly ($P < 0.05$) different from the PGL-SLNopt dispersion stored at 25 °C. The initial particle size and EE found to be

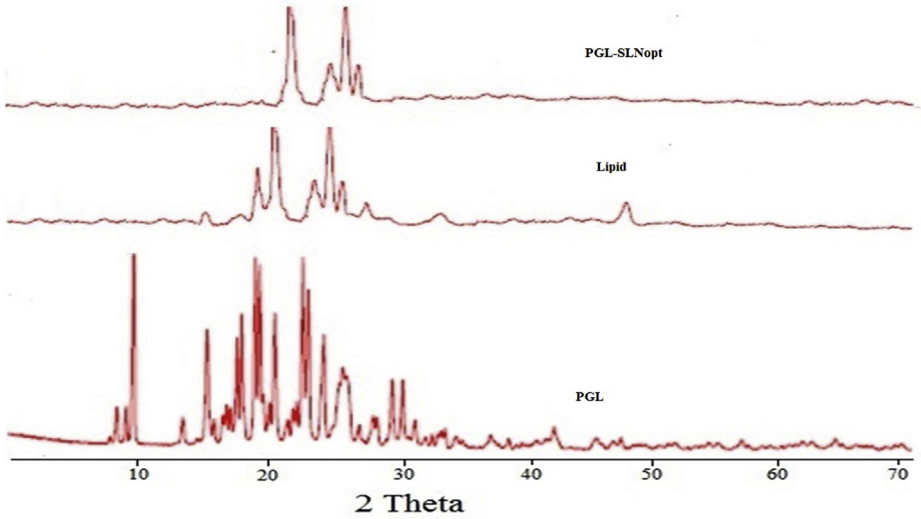

Fig. 7. X-ray diffraction image of PGL, Campritol ATO888 and optimized pioglitazone solid lipid nanoparticles (PGL-SLNopt).

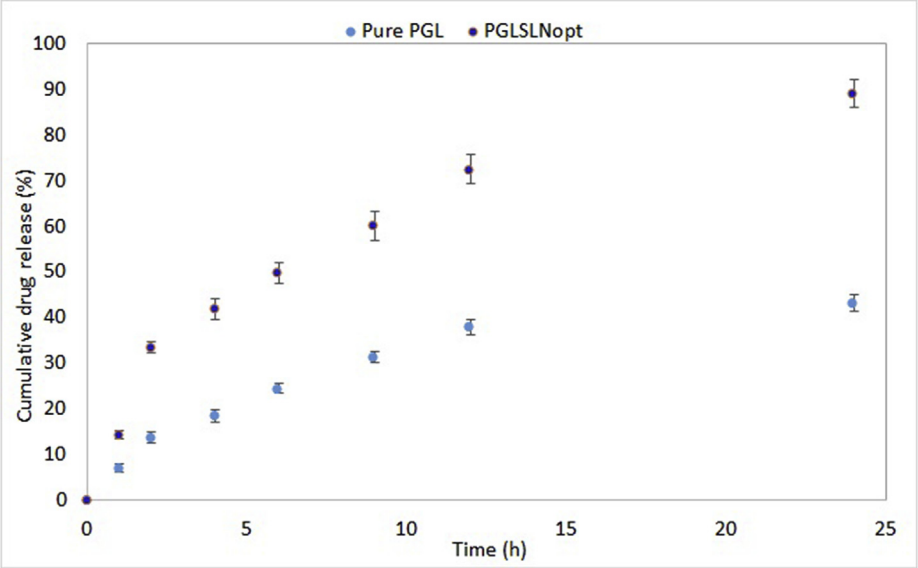

Fig. 8. Comparative *in-vitro* release study of optimized pioglitazone solid lipid nanoparticles (PGL-SLNopt) and pure pioglitazone (PGL).

186.76 ± 4.11 nm and 87.11 ± 3.98%, and after 180-day storage, it showed a significant increase ($P < 0.05$) in particle size (244.87 ± 8.24) and decrease in EE (73.09 ± 3.15%). The variation in the result was found due to, agglomeration of particle and leakage of drug from SLNs at high temperature and also may be due to instability at the higher temperature on long term storage accelerated condition.

4. Conclusion

The PGL-SLNs were developed by hot homogenization method using Compritol® 888 ATO as lipid and tween 80 as surfactant. PGLSLNopt formulation showed the low particle size, high encapsulation efficiency, and optimum PDI as well as zeta potential. The drug release of PGL-SLNopt displayed high and prolonged release of 89.56 ± 3.11%. DSC and XRD study of PGL-SLNopt formulation revealed PGL losses the crystallinity and transformed into an amorphous state. PGL-SLNopt showed significantly ($P < 0.05$) higher hypoglycemic activity than pure PGL dispersion. It confirms that PGL has higher therapeutic effectiveness after encapsulating into SLN formulation.

CRediT authorship contribution statement

Sharma Shaveta: Investigation, Formal analysis. **Jyoti Singh:** Supervision, Data curation, Conceptualization. **Muhammad Afzal:** Writing - original draft. **Rupinder Kaur:** Supervision. **Syed Sarim Imam:** Software, Writing - review & editing. **Nabil K. Alruwaili:** Writing - review & editing. **Khalid Saad Alharbi:** Writing - review & editing. **Nasser Hadal Alotaibi:** Writing - review & editing. **Mohammed Salem Alshammari:** Writing - review & editing. **Imran Kazmi:** Writing - review & editing. **Mohd Yasir:** Writing - review & editing. **Amit Goyel:** Conceptualization. **Ameeduzzafar:** Writing - original draft, Software.

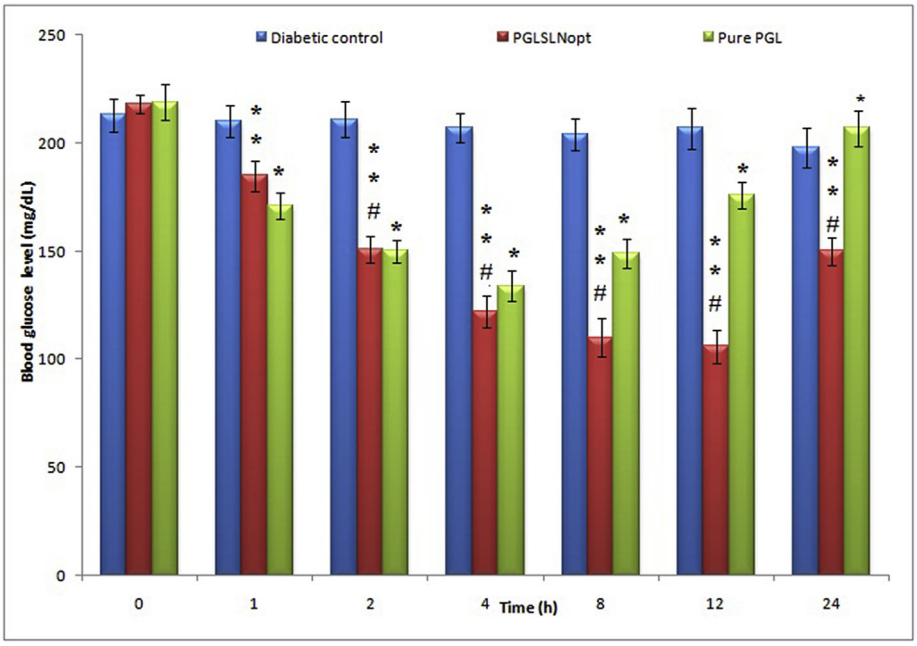

Fig. 9. Comparative *in–vivo* antidiabetic image of pure PGL and optimized pioglitazone solid lipid nanoparticles (PGL-SLNopt).

Table 4
Comparative serum level of biochemical estimation in different treated groups.

Group	TC (mg/dl) (Mean ± SD)	TG (mg/dl) (Mean ± SD)	HDL (mg/dl) (Mean ± SD)	UA (mg/dl) (Mean ± SD)	Urea (mg/dl) (Mean ± SD)	SGPT (U/dl) (Mean ± SD)	SGOT (U/dl) (Mean ± SD)
Normal control	50.2 ± 0.63	31.35 ± 0.32	45.51 ± 1.65	1.40' ± 0.48	31.9 ± 1.98	46.45 ± 2.81	50.87 ± 2.76
Diabetic control	114.45 ± 1.23	52.42 ± 1.23	23.67 ± 2.34	2.89 ± 0.49	57.76 ± 1.65	60.74 ± 2.36	78.7 ± 2.76
Pure PGL	79.26 ± 0.84	44.21 ± 0.76	32.83 ± 2.1	1.91 ± 0.89	48.72 ± 1.27	48.6 ± 1.86	65.54 ± 3.53
PGL-SLNopt	59.24 ± 0.49***	35.32 ± 0.73***	36.12 ± 1.05***	1.65 ± 0.59*	42.5 ± 1.21**	45.0 ± 1.43**[8]	54.76 ± 2.39***

TC: Total cholesterol, TG: Triglycerides, HDL: high-density lipoproteins, UA: Uric acid, SGPT: Serum glutamic pyruvic transaminase, SGOT: Serum glutamic oxaloacetic transaminase. ***P < 0.001 compared with Diabetic control and Pure PGL; **P < 0.01 compared with Diabetic control; # ns P > 0.05 compared with PGL-SLNs.

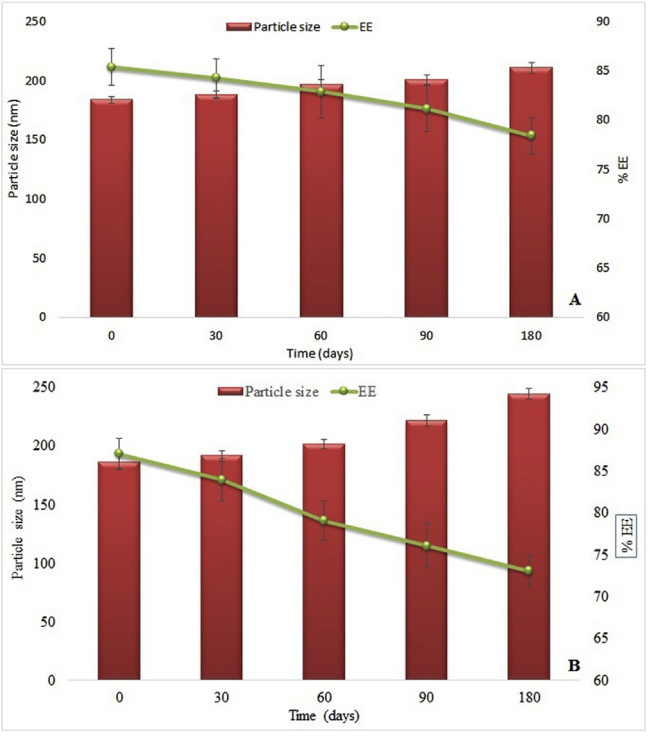

Fig. 10. Stability study of optimized pioglitazone solid lipid nanoparticles (PGL-SLNopt) at different temperature.

Declaration of competing interest

None.

Acknowledgement

Authors **(Shaveta Sharma, Jyoti Singh, Rupinder Kaur, Amit Goyal)** would like to thanks the management of Chandigarh College of Pharmacy, Landran and Punjab University for providing facilities to do this research work.

Appendix A. Supplementary data

Supplementary data to this article can be found online at https://doi.org/10.1016/j.jddst.2020.101674.

References

[1] S. Wild, G. Roglic, A. Gree, R. Sicree, H. King, Global prevalence of diabetes: estimates for the year 2000 and projections for 2030, Diabetes Care 27 (2004) 1047–1053.
[2] T.A. Zelniker, S.D. Wiviott, I. Raz, K. Im, E.L. Goodrich, M.P. Bonaca, O. Mosenzon, E.T. Kato, et al., SGLT2 inhibitors for primary and secondary prevention of cardiovascular and renal outcomes in type 2 diabetes: a systematic review and meta-analysis of cardiovascular outcome trials, Lancet 393 (10166) (2019) 31–39.
[3] H. Kolb, S. Martin, Environmental/lifestyle factors in the pathogenesis and prevention of type 2 diabetes, BMC Med. 15 (2017) 131.
[4] S. Canivell, M. Mata Cases, J. Real, J. Franch-Nadal, B. Vlacho, K. Khunti, M. Gratacòs, D. Mauricio, Glycaemic control after treatment intensification in patients with type 2 diabetes uncontrolled on two or more non-insulin antidiabetic drugs in a real-world setting, Diabetes ObesMetab. 21(6) 20191373-20191380 .
[5] S.A. Mosure, J. Shang, J. Eberhardt, R. Brust, J. Zheng, P.R. Griffin, S. Forli, D.J. Kojetin, Structural basis of altered potency and efficacy displayed by a major in vivo metabolite of the antidiabetic PPARγ drug pioglitazone, J. Med. Chem. 62 (4) (2019) 2008–2023.
[6] S. Wittayalertpanya, S. Chompootaweep, N. Thaworn, The pharmacokinetics of pioglitazone in Thai healthy subjects, J. Med. Assoc. Thai. 89 (2006) 2116–2222.
[7] A. A Elbary, M.A. Kassem, M.M. Abou Samra, R.M. Khalil, Formulation and hypoglycemic activity of pioglitazone-cyclodextrin inclusion complexes, Drug Discov. Ther. 2 (2008) 94–107.
[8] B.M. Boddupalli, P. Masana, R.N. Anisetti, S.V. Kallem, B. Madipoju, Formulation and evaluation of pioglitazone loaded bovine serum albumin nanoparticles along with piperine, Drug Invent. Today 5 (2013) 212–215.
[9] P.S. Prasad, S.S. Imam, M. Aqil, Y. Sultana, A. Ali, QbD-based carbopol transgel formulation: characterization, pharmacokinetic assessment and therapeutic efficacy in diabetes, Drug Deliv. 23 (3) (2016) 1047–1056.
[10] S. Alam, M. Aslam, A. Khan, S.S. Imam, M. Aqil, Y. Sultana, A. Ali, Nanostructured lipid carriers of pioglitazone for transdermal application: from experimental design to bioactivity detail, Drug Deliv. 23 (2) (2016) 601–609.
[11] W. He, Y. Li, R. Zhang, Z. Wu, L. Yin, Gastro-floating bilayer tablets for the sustained release of metformin and immediate release of pioglitazone: preparation and in vitro/in vivo evaluation, Int. J. Pharm. 476 (2014) 223–231.
[12] P. Hyma, K. Abbulu, Formulation and characterisation of self-microemulsifying drug delivery system of pioglitazone, Biomed. Prev. Nutr. 3 (2013) 345–350.
[13] C.B. Spinks, A.S. Zidan, M.A. Khan, M.J. Habib, P.J. Faustino, Pharmaceutical characterization of novel tenofovir liposomal formulations for enhanced oral drug delivery: in vitro pharmaceutics and Caco-2 permeability investigations, Clin. Pharmacol. 9 (2017) 29–38.
[14] B.B. Alsulays, M.K. Anwer, G.A. Soliman, S.M. Alshehri, E.S. Khafagy, Impact of penetratin stereochemistry on the oral bioavailability of insulin-loaded solid lipid nanoparticles, Int. J. Nanomed. 14 (2019) 9127–9138.
[15] A. Mishra, S.S. Imam, M. Aqil, A. Ahad, Y. Sultana, Ameeduzzafar, A. Ali, Carvedilol nano lipid carriers: formulation, characterization and in-vivo evaluation, Drug Deliv. 23 (4) (2016) 1486–1494.
[16] A. Paudel, Ameeduzzafar, S.S. Imam, M. Fazil, S. Khan, A. Hafeez, F.J. Ahmad, A. Ali, Formulation and optimization of candesartan cilexetil nano lipid carrier: in vitro and in vivo evaluation, Curr. Drug Deliv. 14 (7) (2017) 1005–1015.
[17] V. Mishra, K.K. Bansal, A. Verma, N. Yadav, S. Thakur, K. Sudhakar, J.M. Rosenholm, Solid lipid nanoparticles: emerging colloidal nano drug delivery systems, Oct 18, Pharmaceutics 10 (4) (2018) pii: E191.
[18] P. Ganesan, P. Ramalingam, G. Karthivashan, Y.T. Ko, D.K. Choi, Recent developments in solid lipid nanoparticle and surface-modified solid lipid nanoparticle delivery systems for oral delivery of phyto-bioactive compounds in various chronic diseases, Int. J. Nanomed. 13 (2018) 1569–1583.
[19] B. Stella, E. Peira, C. Dianzani, M. Gallarate, L. Battaglia, C.L. Gigliotti, E. Boggio, U. Dianzani, F. Dosio, Development and characterization of solid lipid nanoparticles loaded with a highly active doxorubicin derivative, Nanomaterials 8 (2) (2018) pii: E110.
[20] N.L. Trevaskis, L.M. Kaminskas, C.J. Porter, From sewer to saviour - targeting the lymphatic system to promote drug exposure and activity, Nat. Rev. Drug Discov. 14 (2015) 781–803.
[21] C.J.H. Porter, N.L. Trevaskis, W.N. Charman, Lipids and lipid-based formulations: optimizing the oral delivery of lipophilic drugs, Nat. Rev. Drug Discov. 6 (2007) 231–248.
[22] J.S. Negi, P. Chattopadhyay, A.K. Sharma, V. Ram, Development of solid lipid nanoparticles (SLNs) of lopinavir using hot self nano-emulsification (SNE) technique, Eur. J. Pharmaceut. Sci. 48 (1–2) (2013) 231–239.
[23] C. Carbone, B. Tomasello, B. Ruozi, M. Renis, G. Puglisi, Preparation and optimization of PIT solid lipid nanoparticles via statistical factorial design, Eur. J. Med. Chem. 49 (2012) 110–117.
[24] M.D. Ansari, S. Ahmed, S.S. Imam, I. Khan, S. Singhal, M. Sharma, Y. Sultana, CCD based development and characterization of nano-transethosome to augment the antidepressant effect of agomelatine on Swiss albino mice, J. Drug Deliv. Sci.

Technol. 54 (2019) 101234.
[25] Khaled M. Hosny, Khalid M. El-Say, Hal M. Alkhalidi, Quality by design approach to screen the formulation and process variables influencing the characteristics of carvedilol solid lipid nanoparticles, J. Drug Deliv. Sci. Technol. 45 (2018) 168–176.
[26] B. Gidwani, A. Vyas, Preparation, characterization, and optimization of altretamine-loaded solid lipid nanoparticles using Box-Behnken design and response surface methodology, Art, Cells Nanomed Biotechnol 44 (2) (2016) 571–580.
[27] G. Amasya, B. Aksu, U. Badilli, A. Onay-Besikci, N. Tarimci, QbD guided early pharmaceutical development study: production of lipid nanoparticles by high pressure homogenization for skin cancer treatment, Int. J. Pharm. 563 (2019) 110–121.
[28] Ameeduzzafar, J Ali, A Bhatnagar, N. Kumar, AAli, Chitosan nanoparticles amplify the ocular hypotensive effect of carteolol in rabbits, Int. J. Biol. Macromol. 65 (2014) 479–491.
[29] Ameeduzzafar, S.S. Imam, S.N. Abbas Bukhari, J. Ahmad, A. Ali, Formulation and optimization of levofloxacin loaded chitosan nanoparticle for ocular delivery: in-vitro characterization, ocular tolerance and antibacterial activity, Int. J. Biol. Macromol. 108 (2018) 650–659.
[30] B.M. Aljaeid, K.M. Hosny, Miconazole-loaded solid lipid nanoparticles: formulation and evaluation of a novel formula with high bioavailability and antifungal activity, Int. J. Nanomed. 11 (2016) 441–447.
[31] X.X. Guo, Y. Wang, K.B.P. Wang Ji, F. Zhou, Stability of a type 2 diabetes rat model induced by high-fat diet feeding with low-dose streptozotocin injection, J. Zhejiang Univ. - Sci. B. 19 (7) (2018) 559–569.
[32] P. Trinder, Determination of glucose in blood using glucose oxidase with an alternative oxygen acceptor, Ann. Clin. Biochem. 6 (1969) 24.
[33] ICH Topic Q 1 A (R2), Stability Testing of New Drug Substances and Products, (August 2003) CPMP/ICH/2736/99.
[34] M. Yasir, U.V.S. Sara, I. Chauhan, P.K. Gaur, A.P. Singh, D. Puri, Ameeduzzafar, Solid lipid nanoparticles for nose to brain delivery of donepezil: formulation, optimization by Box- behnken design, in vitro and in vivo evaluation, art, Cells Nanomed. and Biotech. 46 (8) (2018) 1838–1852.
[35] T. Helgason, T.S. Awad, K. Kristbergsson, D.J. McClements, J. Weiss, Effect of surfactant surface coverage on formation of solid lipid nanoparticles (SLN), J. Colloid Interface Sci. 334 (1) (2009) 75–81.
[36] A.K. Kushwaha, P.R. Vuddanda, P. Karunanidhi, S.K. Singh, S. Singh, Development and evaluation of solid lipid nanoparticles of raloxifene hydrochloride for enhanced bioavailability, 2013, BioMed Res. Int. (2013) 584549.
[37] M.S. Baig, A. Ahad, M. Aslam, S.S. Imam, M. Aqil, A. Ali, Application of Box-Behnken design for preparation of levofloxacin-loaded stearic acid solid lipid nanoparticles for ocular delivery: optimization, in vitro release, ocular tolerance, and antibacterial activity, Int. J. Biol. Macromol. 85 (2016) 258–270.
[38] B. Gidwani, A. Vyas, Preparation, characterization, and optimization of altretamine-loaded solid lipid nanoparticles using Box-Behnken design and response surface methodology, Artif Cells Nanomed, Biotechnol. 44 (2) (2016) 571–580.
[39] S.Z.H. Rizvi, F.A. Shah, N. Khan, I. Muhammad, K.H. Ali, M.M. Ansari, F.U. Din, O.S. Qureshi, K.W. Kim, Y.H. Choe, J.K. Kim, A. Zeb, Simvastatin-loaded solid lipid nanoparticles for enhanced anti-hyperlipidemic activity in hyperlipidemia animal model, Int. J. Pharm. 560 (2019) 136–143.
[40] Ameeduzzafar, I. El-Bagory, N.K. Alruwaili, M.H. Elkomy, J. Ahmad, M. Afzal, N. Ahmad, M. Elmowafy, K.S. Alharbi, M.S. Alam, Development of novel dapagliflozin loaded solid self-nanoemulsifying oral delivery system: physiochemical characterization and in vivo antidiabetic activity, J. Drug Deliv. Sci. Technol. 54 (2019) 101279.
[41] N. Dudhipala, K. Veerabrahma, Candesartan cilexetil loaded solid lipid nanoparticles for oral delivery: characterization, pharmacokinetic and pharmacodynamic evaluation, Drug Deliv. 23 (2) (2016) 395–404.
[42] S. Pandey, P. Patel, A. Gupta, Novel solid lipid nanocarrier of glibenclamide: a factorial design approach with response surface methodology, Curr. Pharmaceut. Des. 24 (16) (2018) 1811–1820.
[43] L.M. Gonçalves, F. Maestrelli, L. Di Cesare Mannelli, C. Ghelardini, A.J. Almeida, P. Mura, Development of solid lipid nanoparticles as carriers for improving oral bioavailability of glibenclamide, Eur. J. Pharm. Biopharm. 102 (2016) 41–50.
[44] S.M. Sefidgar, M. Ahmadi-Hamedani, A. J Javan, R. N Sani, A.J. Vayghan, Effect of crocin on biochemical parameters, oxidative/antioxidative profiles, sperm characteristics and testicular histopathology in streptozotocin-induced diabetic rats, Avicenna J Phytomed 9 (4) (2019) 347–361.
[45] S.A. Nabi, R.B. Kasetti, S. Sirasanagandla, T.K. Tilak, M.V. Kumar, C.A. Rao, Antidiabetic and antihyperlipidemic activity of Piper longum root aqueous extract in STZ- induced diabetic rats, BMC Compl. Alternative Med. 13 (37) (2013) 2–9.